A GENUINELY MULTIDISCIPLINARY JOURNAL

CHEMPLUSCHEM

CENTERING ON CHEMISTRY

Accepted Article

Title: Tetrahedral Silicon-Centered Dibenzoylmethanatoboron Difluorides: Synthesis, Crystal Structure and Photophysical Behavior in Solution and Solid State

Authors: Yuriy Kononevich, Maxim M. Temnikov, Alexander A. Korlyukov, Alexander D. Volodin, Pavel V. Dorovatovskii, Viacheslav A. Sazhnikov, Andrey A. Safonov, Dmitriy S. Ionov, Anatoly A. Ivanov, Nikolay M. Surin, Evgeniya A. Svidchenko, and Aziz M. Muzafarov

To be cited as: *ChemPlusChem* 10.1002/cplu.201900732

Link to VoR: http://dx.doi.org/10.1002/cplu.201900732

A Journal of

ChemPubSoc Europe

WILEY-VCH

www.chempluschem.org

Tetrahedral Silicon-Centered Dibenzoylmethanatoboron Difluorides: Synthesis, Crystal Structure and Photophysical Behavior in Solution and Solid State

Yuriy N. Kononevich,*[a] Maxim N. Temnikov,[a] Alexander A. Korlyukov,[a][b] Alexander D. Volodin,[a] Pavel V. Dorovatovskii,[c] Viacheslav A. Sazhnikov,[d][e] Andrey A. Safonov,[d] Dmitriy S. Ionov,[d] Anatoly A. Ivanov,[d] Nikolay M. Surin,[f] Evgeniya A. Svidchenko,[f] and Aziz M. Muzafarov *[a][f]

Abstract: Four novel tetrahedral silicon-centered derivatives of dibenzoylmethanatoboron difluoride ($DBMBF_2$) were synthesized and characterized. Their structural and optical features both in solution and solid state were investigated using X-ray crystallography, steady and time-dependent spectroscopy, and DFT-based calculations. In dilute solutions, the molar absorption coefficient increases with increasing the number of $DBMBF_2$ fragments in a molecule from 40500 to 175200 $M^{-1}cm^{-1}$, while, in contrast, the nonradiative rate constant of fluorescence decay decreases from 0.49 to 0.34. In the solid state, absorption and emission spectra depend on the degree of crystallinity and microcrystal size. Tris-$DBMBF_2$ derivative forms fully overlapping dimeric structures exhibiting excimer-like fluorescence, which is well predicted by the quantum-chemical calculations. Mono-$DBMBF_2$ derivative exhibits fully reverse mechanofluorochromic behavior.

Introduction

In recent years there has been an intense interest in the design and synthesis of tetrahedral silicon-centered organic molecules that can be used in numerous applications. These molecules based on silane core have been proved to be fascinating building blocks for constructing various 3D porous metal-organic frameworks (MOFs),[1–3] dynamic covalent frameworks (DCFs)[4,5] and element-organic framework (EOF).[6] Silicon-containing monomers with tetrahedral and triangular-pyramidal shapes can be utilized for obtaining porous resins[7,8] and films.[9] Tetrahedral scaffold-type silicon-containing molecules can be used as rigid linkers for immobilization of various catalysts.[10–15] Tripod-shaped oligo(p-phenylene)s joined together by a single silicon atom can be utilized as anchors for the functionalization of different surfaces by various chromophores.[16–19] Dendrimer-like structures based on different silanes[20,21] in particular organosilicon molecular antennas[22] have been obtained. Tetrahedral silicon-centered cyano-functionalized silanes with high thermal stability can be used as fluorescent sensors for diphenylamine detection[23] and flexible network based on tetrahedral silicon-centered structures can be used for fluorescence sensing of aromatic compounds.[24]

Triphenylsilylphenyl and triphenylsilylphenyl(ethynyl) bulky substituents included into p-conjugated systems can suppress π–π interaction due to their steric hindrance[25,26] and, thus, lead to an improvement of optoelectronic properties such compounds.[27] The incorporation of silicon atoms into p-conjugated systems can decrease LUMO energy levels essentially due to a strong (Si-C)-p* hyperconjugation effect. Thus, numerous luminescent materials based on tetrahedral silicon-centered organic molecules due to their potential application as well as organic light emitting devices (OLEDs) were obtained and investigated.[28–45]

It is well known that boron difluoride complexes such as $DBMBF_2$, BODIPY and others possess valuable photophysical / photochemical properties and are promising objects in the development of new fluorescent materials for organic electronics and photonics.[46–48] These compounds exhibit large extinction coefficients and two-photon absorption cross section, show intense fluorescence with high quantum yields both in solutions and in the solid state, and also possess mechanofluorochromic properties.[49–51] Such boron complexes can be utilized as various fluorescent sensors.[52] for example for detecting of BTEX.[53–61] It should be noted that such BTEX detection is based on the formation of fluorescent exciplexes between $DBMBF_2$ and benzene derivatives. However, at relatively high concentrations of $DBMBF_2$ required for sensitive materials, a competitive reaction of the formation of fluorescent excimers between two adjacent $DBMBF_2$ molecules can occur. It can be expected that the use of silicon-centered derivatives of $DBMBF_2$ with tetrahedral or triangular-pyramidal shapes can be used to obtain sensitive materials with a reduced ability to form similar dimeric associations of $DBMBF_2$ in the ground or excited states. Also note that derivatives of various silicon-cored compounds

[a] Dr. Yuriy N. Kononevich, Dr. Maxim N. Temnikov, Prof. Alexander A. Korlyukov, Alexander D. Volodin, Prof. Aziz M. Muzafarov.
A.N. Nesmeyanov Institute of Organoelement Compounds, Russian Academy of Sciences
119991 Moscow, Russian Federation
E-mail: kononevich.yuriy@gmail.com
[b] Prof. Alexander A. Korlyukov
Pirogov Russian National Research Medical University
117997 Moscow, Russian Federation
[c] Pavel V. Dorovatovskii
National Research Center “Kurchatov Institute”
123098 Moscow, Russian Federation
[d] Dr. Viacheslav A. Sazhnikov, Dr. Andrey A. Safonov, Dmitriy S. Ionov, Dr. Anatoly A. Ivanov
Photochemistry Center, FSRC “Crystallography and Photonics”, Russian Academy of Sciences
1119421 Moscow, Russian Federation
[e] Dr. Viacheslav A. Sazhnikov
Moscow Institute of Physics and Technology (State University)
141707 Dolgoprudny, Russian Federation
[f] Dr. Nikolay M. Surin, Evgeniya A. Svidchenko, Prof. Aziz M. Muzafarov
N.S. Enikolopov Institute of Synthetic Polymeric Materials, Russian Academy of Sciences
117393 Moscow, Russian Federation

Supporting information for this article is given via a link at the end of the document.

typically exhibit higher absorption coefficients and fluorescence quantum yields as compared to their parent molecules. It was interesting to study how these effects which are of significant value for fluorescent molecular sensors can be characteristic of silicon-centered $DBMBF_2$ derivatives. In addition, there is a great deal of interest in understanding the fluorescence properties of dimer-type structures in $DBMBF_2$-based crystals.

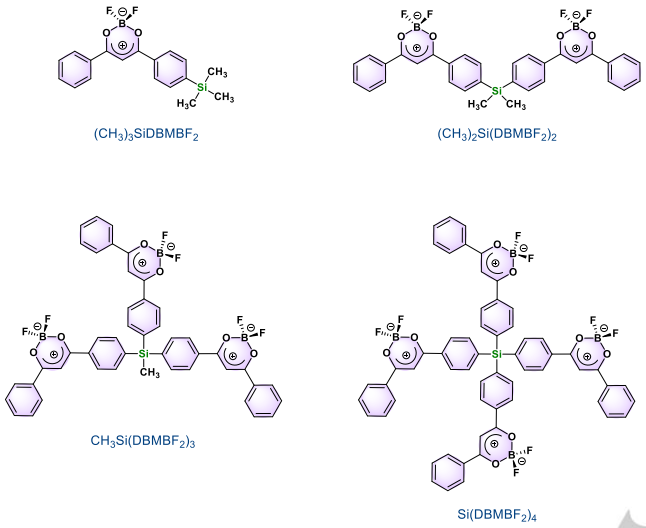

Figure 1. Tetrahedral silicon-centered derivatives of diketonatoboron difluoride.

In this paper, we present a series of novel silicon-centered dendritic diketonatoboron difluorides (Figure 1). The crystal structure of synthesized compounds was determined by X-ray diffraction analysis and their photophysical properties were studied both in solution and in the solid state. In particular, it was observed that $(DBMBF_2)_3SiCH_3$ forms completely overlapped excimer-like structures in the crystalline state, whereas $DBMBF_2Si(CH_3)_3$ exhibits reversible mechanofluorochromism.

Results and Discussion

Synthesis of tetrahedral Si-centered diketonatoboron difluorides. The organosilicon derivatives of diketonatoboron difluorides **7 a-d** were synthesized according to the route outlined in Scheme 1. The starting compound in the synthesis of **7 a-d** was 4-bromoacetophenone **1**, the carbonyl group of which was protected with a dioxolane group. The reaction was carried out by a known procedure, namely by boiling of 4-bromoacetophenone **1** with ethylene glycol in toluene in the presence of TsOH as a catalyst and with a Dean-Stark trap. The product **2** was purified by a recrystallization from hexane.

In the next stage the compound **2** was treated with equimolar amount of n-BuLi in THF at -80 °C and then with corresponding chlorosilane. After the isolation and purification by the recrystallization from hexane compounds **4 a-d** were obtained with good yields.

Organosilicon derivatives of acetophenone **5 a-d** were obtained by removing the protecting group from **4 a-d** in boiled aqueous acetone in the presence of TsOH. After isolation **5 b-d** as colorless crystals and **5 a** as a colorless oil were obtained. Further, by the action with LiHMDS (solution in THF) on the corresponding acetophenones **5 a-d**, and then addition of benzoylchloride lead to obtain of organosilicon 1,3-diketones **6 a-d**, which were purified by column chromatography on silica with toluene as an eluent. It should be noted that in the case of Claisen condensation between corresponding acetophenones **5 a-d** and ethylbenzoate in THF solution with NaH as a base no positive results were obtained, since the cleavage of silicon-carbon bond was observed.

The final stage in the synthesis of tetrahedral silicon-centered derivatives of dibenzoylmethanatoboron difluoride **7 a-d** (Figure 1) was the reaction between 1,3-diketones **6 a-d** and boron trifluoride diethyl etherate in dichloromethane. In the case of **7 a** and **7 c** after the completion of reaction, the solvent was removed in vacuo and the residue was recrystallized from toluene. In the case of **7 b** and **7 d** products were collected by filtration and didn't need any further purification. Boron difluoride complexes **7 a-d** were obtained as yellow substances. All obtained compounds were characterized by ^{1}H, ^{13}C, ^{19}F, ^{29}Si NMR, IR, MS, and elemental analysis (Supporting information).

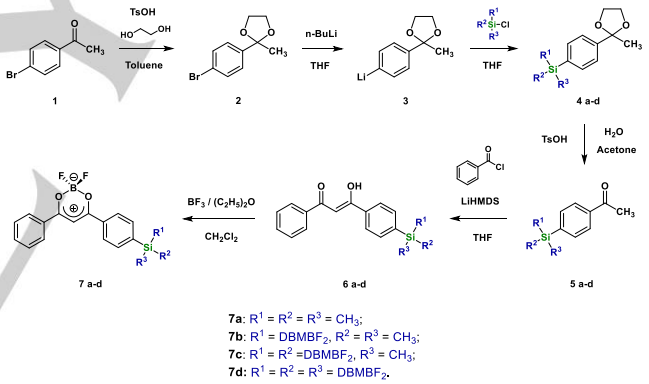

Scheme 1. Synthesis of organosilicon derivatives of $DBMBF_2$ **7 a-d**..

X-ray analysis. Compounds **7 c and 7 d** crystallized in monoclinic cells, while **7 a** and **7 b** form triclinic ones. Analysis of the crystal packing has shown that almost all phenyl rings and boron-containing rings engaged in stacking interactions (Supporting information). Phenyl cycles in **7 c** participate in stacking interaction with the same fragments of adjacent molecules thus forming dimers (Figure 2, main text and Figures S96-S98, Supporting information). The strongest stacking in this crystal is formed by the rings C10C-C15C and C10D-C15D (interplanar distance is equal to 3.322 (9) Å). Crystal **7 c** is colored yellow while all other crystals studied by X-ray diffraction are light-yellow. The F1A atom in the **7 c** crystal also forms a hydrogen bond of medium strength with the molecule $CHCl_3$ (donor-acceptor distance equal 3.086(17) Å) (Figure 2).

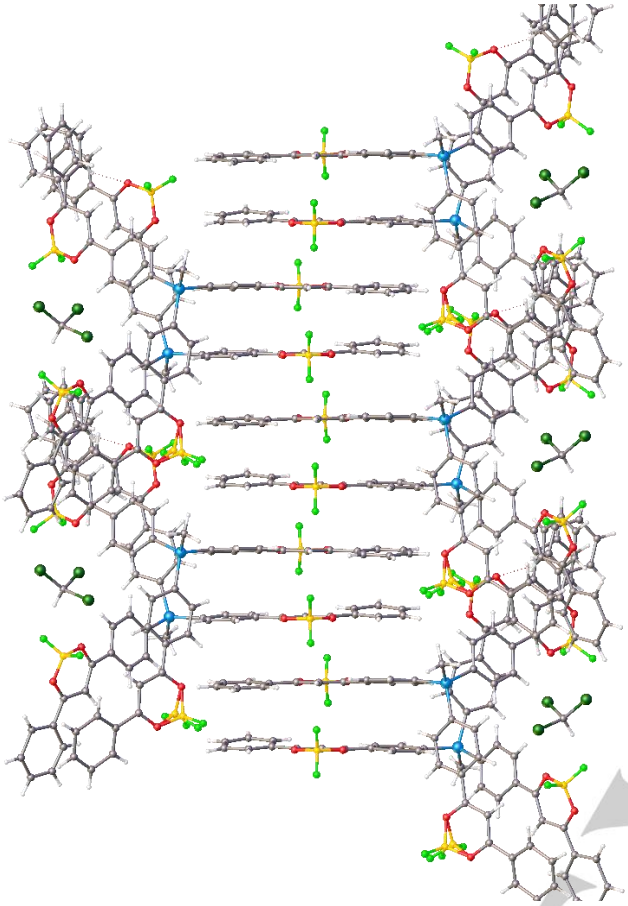

Figure 2. Molecular packing of **7 c** in the crystal lattice. C (grey), O (red), Si (blue), H (white), B (yellow), F (green), Cl (dark green).

In all compounds there are contacts H···F, but except for the above-described contact H3···F1A in **7 c**, they are weak (corresponding interatomic distance more than 3.2 Å). Boron-containing rings in the compounds **7 a-d** are close to plane conformation.

Among studied compounds it is easy to reveal the compounds with very similar crystal packing. In other words, crystal packing for pairs of compounds differing only by presence of the BF_2 fragment does not differ much. For example, in **6 d** and **7 d** the same space group and packing motives were revealed (Figures S90, S100, Supporting information). The crystals consist of stacks along the *b* axis of unit cell, in which the molecules are mainly connected by π-stacking. Compounds **6 b** and **7 b** also have a similar packing. Both compounds are packed with stacks that resemble arrows (Figures S88 for **6 b**, S94 for **7 b**, Supporting information). In crystal **7 b** all molecules are orientated in the same direction, while the orientation of **6 b** molecules alternates layer by layer. The dimers of the **7 c** are linked together by π-/dipole-dipole interaction and disposed along c axis, so the interaction with molecules of another dimer is possible (Figure 2). The cycles not participating in this interaction are turned orthogonally to the plane ab. On the other hand, the crystal packing of **6 a** and **7 a** is significantly different.

The crystals **6 a** and **7 a** also has a layered structure. The molecules in both cases are assembled by the π-stacking of the phenyl rings, but the dipole-dipole interaction between boron-containing rings is presented only in **7 a** packing (Figures S86 and S96, Supporting information). The boron ring in the **6 a** crystal interacts with other molecules only by weak hydrogen bonds (C–H···O and C–H···π).

CCDC 1983329 (**6 a**), 1907458 (**6 b**), 1907456 (**6 d**), 1907457 (**7 a**), 1907459 (**7 b**), 1907455 (**7 c**), 1907454 (**7 d**) contain the supplementary crystallographic data for this paper. These data can be obtained free of charge from The Cambridge Crystallographic Data Centre.

Photophysical properties in solution. The photophysical characteristics of the synthesized compounds were measured in dichloromethane solutions and are summarized in Table 1. Normalized electronic absorption and emission spectra of organosilicon derivatives of $DBMBF_2$ **7 a-d** obtained in dichloromethane solution at room temperature are presented in Figure 3.

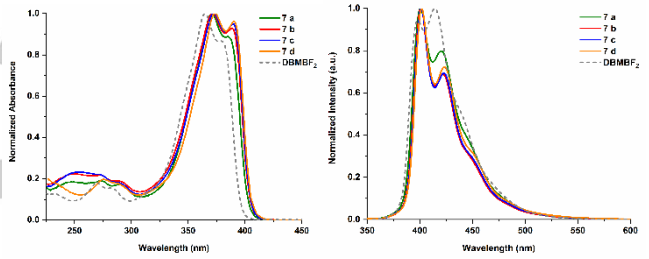

Figure 3. Normalized electronic absorption (left) and emission (λ_{ex} = 371 nm) (right) spectra of organosilicon derivatives of $DBMBF_2$ **7 a-d** in dichloromethane at room temperature. The dye concentration is 1 * 10^{-5} M for all compounds.

Table 1. Optical properties of organosilicon derivatives of $DBMBF_2$ **7 a-d** and unsubstituted $DBMBF_2$ in the solution.[a]

Com-pound	λ_{abs} (nm)	K_{ext} (M^{-1} cm^{-1})	λ_{em} (nm)	Φ_f	0-0 (cm^{-1})	τ_f (ps)	k_{rf} (10^8 s)	k_{nrf} (10^8 s)
7 a	371 (385)	40500	401 (421)	0.49	25400	1000	4.9	5.1
7 b	372 (388)	72900	401 (422)	0.47	25300	946	5	5.6
7 c	373 (390)	101100	401 (423)	0.42	25300	808	5.2	7.2
7 d	374 (390)	175200	402 (423)	0.34	25200	657	5.2	10
$DBMBF_2$	365 (379)	39100	414 (398)	0.20	25700	470[b]	5.5	16

[a] The optical properties were measured in dichloromethane (c = 1 * 10^{-5} M). The wavelengths of the second absorption and fluorescence peak are given in parentheses.
[b] Reference.[46]

The absorption spectra of compounds **7 a-d** dissolved in dichloromethane consist of almost identical structured strong bands with two resolved peaks and shoulders: maxima at 371, 372, 373, 374 nm, second peaks at 385, 388, 390, 390 nm for compounds **7 a**, **7 b**, **7 c** and **7 d**, respectively, and shoulders at about 350 nm (Figure 3). The absorption maxima of compounds **7 a-d** are red-shifted by 6-9 nm in comparison with unsubstituted $DBMBF_2$ and have a similar pattern of band distribution. Data listed in Table 1 show that an increase in the number of $DBMBF_2$

fragments leads to nearly proportional increase of the molar extinction coefficient that is in the range of 40500-175200 $M^{-1}cm^{-1}$ and almost no effect on absorption spectra. Two resolved peaks at 379 and 365 nm and a shoulder at about 350 nm of the parent $DBMBF_2$ are vibronic bands.[62] Obviously, similar peaks for compounds **7 a-d** in the region of 350-390 nm can be attributed to vibronic transitions. It should be noted that the intensity of the second band (at 385-390 nm) increases on going from unsubstituted $DBMBF_2$ and mono-$DBMBF_2$ to tetra-$DBMBF_2$.

The fluorescence spectra of compounds **7 a-d** were measured in dichloromethane solutions ($c = 1 \times 10^{-5}$ M) at room temperature. Figure 3 shows the normalized fluorescence spectra of the parent $DBMBF_2$ and synthesized compounds **7 a-d**, and Figure S107 (Supporting information) shows a photograph of the fluorescence of these compounds in dichloromethane. As can be seen in Figure 3 the emission spectra consist of two bands at about 400 and 420 nm and a shoulder at about 450 nm. Compounds **7 a-d** exhibit higher fluorescence quantum yield than parent $DBMBF_2$ (0.2) that drops on going from mono-chromophoric to tetra-chromophoric derivatives (0.49 → 0.47 → 0.42 → 0.34). Figure S108 (Supporting information) demonstrates the fluorescence decay curves obtained for the compound **7 a-d**. The fluorescence lifetime decreases slightly in this series. The observed changes can be attributed to increasing the rate constants of non-radiative processes, while radiative constants remain almost the same and close to the value obtained for $DBMBF_2$. The main non-radiative decay pathway of $DBMBF_2$ is the internal conversion which is related to the torsion vibrations of phenyl rings.[63,64] The addition of *para*-substituents significantly decreases the non-radiative constant and the decrease is higher for more massive substituents.[46] Thus, the decrease of the non-radiative constant of **7 a** is in a good agreement with this trend. The increase of non-radiative constants observed for **7 b-d** appears to be attributable to changes in vibronic frequencies of the single fluorophore environment due to proximity of other fluorophores.

The obtained results also indicate that the degree of conjugation throughout the molecules is relatively small. Thus, the tetrahedral silicon core does not have significant effect on the electronic properties of studied derivatives, which is consistent with published data on similar compounds.[34]

Photophysical properties in the solid state. Absorption and fluorescence spectra of **7 a-d** were also investigated in the solid state and obtained data are summarized in Table 2. The absorption spectra of microcrystals **7 a-d** were measured in a thin layer on a quartz plate (10×25×1 mm) after grinding to an average thickness < 0.15 μm (microcrystal sizes were evaluated by fluorescent microscopy) (Figure 4). These spectra are very similar to those obtained in the solution and consist of structured strong bands with two resolved peaks and shoulders that are red-shifted by 10-20 nm in comparison with spectra obtained in solution.

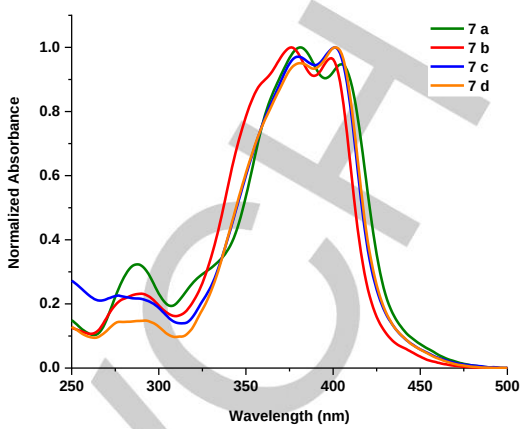

Figure 4. Normalized electronic absorption spectra of organosilicon derivatives of $DBMBF_2$ **7 a-d** in the solid state (grinded microcrystals with average thickness < 0.15 μm).

The fluorescence behavior of compounds **7 a-d** in the solid state at room temperature was also investigated. For this purpose, the fluorescence spectra of solid **7 a-d** with different degree of crystallinity were measured and studied (Figure 5,6, Table 2). Figures 5 shows the normalized fluorescent spectra of solid organosilicon derivatives of $DBMBF_2$ **7 a-d** (grinded microcrystals with average thickness < 0.15 μm, > 0.4 μm, and > 2 μm).

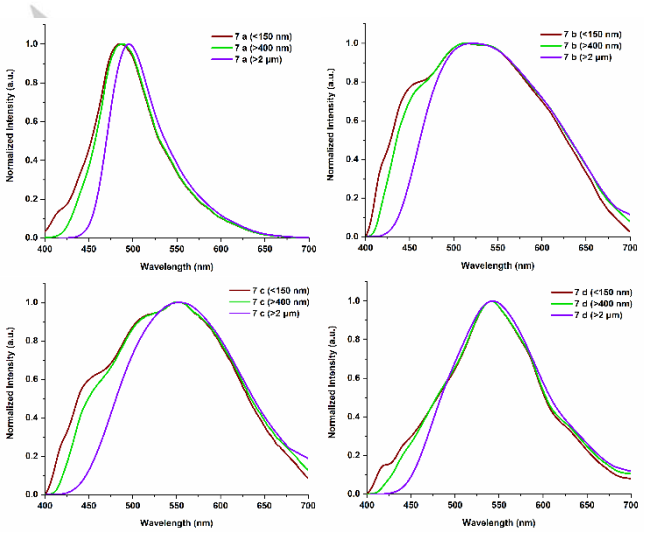

Figure 5. Normalized fluorescence spectra (λ_{ex} = 380 nm) of **7 a-d** in the solid state (grinded microcrystals with average thickness (< 0.15 μm; > 0.4 μm; > 2 μm). Spectra were measured using front-face configuration to minimize the reabsorption.

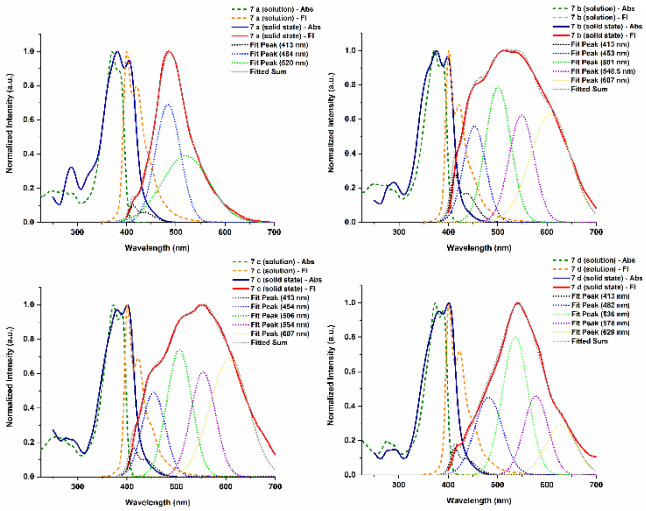

Figure 6. Normalized absorption and fluorescence spectra of **7 a-d** in solution (λ_{ex} = 371 nm) and in the solid state (λ_{ex} = 380 nm) with deconvolution (grinded microcrystals with average thickness < 150 nm). Spectra were measured using front-face configuration to minimize the reabsorption.

Table 2. Optical properties of organosilicon derivatives of $DBMBF_2$ **7 a-d** in the solid state.[a]

Compound	λ_{abs} (nm) Crystals < 0.15 nm	λ_{em} (nm) Crystals < 0.15 nm	λ_{em} (nm) Crystals > 0.4 nm	λ_{em} (nm) Crystals > 2 μm	Φ_f Crystals > 2 μm[b]
7 a	381 (405)	485	487	496	0.37
7 b	376 (399)	514	513	522	0.14
7 c	401 (380)	548	548	553	0.29
7 d	401 (381)	541	541	543	0.10

[a] For measurement of optical properties in the solid state grinded microcrystals with average thickness: a) < 0.15 μm; b) > 0.4 μm; c) > 2 μm) were used. Microcrystal sizes were evaluated by fluorescent microscopy. The wavelengths of the second absorption and fluorescence peaks are given in parentheses.
[b] Taking into account the reabsorption.

Table 3. Fluorescence maxima (nm) and contributions (%) of Gaussian components after decomposition of fluorescence spectra of organosilicon derivatives of $DBMBF_2$ **7 a-d** in the solid state (grinded microcrystals with average thickness < 0.15 μm).

Compound	Peak 1 (nm / %)	Peak 2 (nm / %)	Peak 3 (nm / %)	Peak 4 (nm / %)	Peak 5 (nm / %)
7 a	413 / 4	484 / 46	520 / 50	-	-
7 b	413 / 6	453 / 16	501 / 26	549 / 20	607 / 32
7 c	413 / 4	454 / 15	506 / 25	554 / 21	607 /35
7 d	413 / 5	482 / 22	536 / 37	578 / 20	629 / 16

Table 4. Stokes shifts of components after Gaussian decomposition of fluorescence spectra of organosilicon derivatives of $DBMBF_2$ **7 a-d** in the solid state (grinded microcrystals with average thickness < 0.15 μm).

Compound	Peak 1 (cm^{-1})	Peak 2 (cm^{-1})	Peak 3 (cm^{-1})	Peak 4 (cm^{-1})	Peak 5 (cm^{-1})
7 a	478	4030	5460	-	-
7 b	478	2620	4730	6460	8220
7 c	478	2660	4930	6640	8220
7 d	478	3940	6030	7390	8790

As can be seen in Figure 5 spectra significantly depend on the layer thickness. This can probably be explained by a decrease in the crystallinity of samples and reabsorption. Compounds **7 a-d** exhibit the fluorescence quantum yield in the range of 0.1-0.37 in the solid state. Decompositions of fluorescence spectra of **7 a-d** in the solid state (grinded microcrystals with average thickness < 150 nm) into Gaussian components are presented in Figure 6 and Tables 3,4. Note that the nature of the relationships between the emission properties and crystalline structures of organic luminescent compounds is a controversial matter. Recently, the relationship between the crystal-packing of various alkyl- and silyl-substituted dibenzoylmethanatoboron difluoride derivatives were analyzed in detail by Ikeda and co-workers.[65,66] The authors pointed out that solid state luminescence of $DBMBF_2$ derivatives depends on packaging and particularly on the relative distance between molecules which determines the relative position of chelate and phenyl rings of two molecules in the crystal cell. Three types of packaging were identified. The first packaging corresponds to negligible overlap of phenyl rings with blue luminescence around 450 nm. The second packaging corresponds to overlap of phenyl rings with yellow luminescence around 510 nm and the last is corresponds to overlap of phenyl and chelate ring with blue luminescence around 480 nm. In our case the observed peaks in an amorphous state can be attributed to these packaging. Peak 1 can be attributed to the noninteracting molecules, peak 3 to overlap of phenyl rings, peak 2 to overlap of phenyl and chelate rings. The peak 4 in this case can be attributed to full overlap of the molecules in the face-to-face pairs discussed below in the next section. The peak 5 seems to arise due to non-gaussian form of the discussed luminescence.

Computational studies. The understanding of the properties of excimers in molecular crystals is one of the most interesting problems in solid state chemistry. As reported by Tohnai et al.[67] the π–π stacking arrangement of aromatic molecules (in particular, anthracene-based fluorophores) in the crystalline state can lead to the formation of both excimers as well as unusual excited oligomers. Although the concept of fluorescent multimers of $DBMBF_2$ was proposed and elaborated in detail in the works mentioned above,[65,66] the authors noted that there remains a possibility that the fluorescence emission may be assigned to excimers. We decided to partially explore this possibility. The crystal structures of tri-$DBMBF_2$-substituted silane **7 c** with three $DBMBF_2$ moieties involves $DBMBF_2$ fragments arranged as stacked fully overlapping face-to-face pairs (Figure 2). This structure is very close to the structure

which is considered to be the main one when excimers are formed in solutions. Excimer-like fluorescence of this crystal indicates that the molecular pair form an excimer-like structure at the excitation. To simulate this theoretically, we carried out the quantum-chemical calculation of a pair of $DBMBF_2$ fragments in the excited state. The fragment involved the Si atom of the initial silane terminated by hydrogens. For excited state structures and emission spectra we used combined procedure proposed earlier for exciplexes of $DBMBF_2$ with methylbenzenes.[68]

Geometry optimization in the excited state was performed using the CIS-D method including the Grimme's dispersion correction with the double-zeta def2-SVP basis set. Positions of fluorescence bands were calculated as electronic transition energies at the geometries optimized for the excited state by the TDDFT method with the double-hybrid functional mPW2PLYP and the triple-zeta def2-TZVP basis set. To simulate geometrical constraints imposed by the crystal structure, positions of the Si atoms and terminating hydrogens were fixed in the optimization procedure.

The distance between the nearly parallel fragments in the crystal structure is 3.30–3.38 A. According to calculations, in the excimer-like moiety, the distance between the planes of diketonate cycles decreased to 2.58–2.70 A. The calculated position of the fluorescence band (electronic transition energy at the geometry optimized for the excited state) was about 570 nm (2.18 eV). This is in the excellent agreement with the position of excimer-like band in the spectra of **7 c**. The calculations clearly demonstrate that the observed redshift of the excimer emission is due to the large geometrical change upon the electronic transition (Figures S119, Supporting information).

As shown in Figures S118 (Supporting information) all the crystal-packing structures of silicon-centered derivatives of $DBMBF_2$ are characterized by overlap of the π-orbitals of the phenyl rings and central boron-containing rings of two adjacent molecules. Several modes of molecular overlap observed for the crystalline state of compounds **7 a-d** require more thorough theoretical consideration. We believe that our approach provides a reliable tool for detailed understanding of optical properties of such structures.

Mechanofluorochromic properties. As mentioned above, all synthesized compounds **7 a-d** in the solid state exhibit fluorescent properties. As-synthesized crystals **7 a** show greenish blue (λ_{em} = 486 nm), **7 b** show light blue (λ_{em} = 474 nm), **7 c** show deep yellow (λ_{em} = 571 nm) and **7 d** show blue (λ_{em} = 473 nm) fluorescence at the excitation by light with 365 nm wavelength (Figures 7,8). According to X-ray data, the fluorescence of **7 a,b,d** is in a blue region due to the weaker π-π-interaction between chromophores in the crystal. In contrast, **7 c** has yellow fluorescence. As discussed above, all $DBMBF_2$ fragments in **7 c** have strong stacking between all chromophores in the crystal. After excitation, each fragment can form a highly fluorescent excimer with the nearest fragment located in the most favorable manner. As mentioned above, such excimers can fluoresce in the yellow region of the spectrum. The process of $DBMBF_2$ excimer formation at the excitation is well known for $DBMBF_2$ derivatives in the highly concentrated solution and in the amorphous state.[69]

Table 5. Optical properties of organosilicon derivatives of diketonatoboron difluorides **7 a-d** in solid state before and after grinding.

Compound	λ_{em} before grinding (nm)	λ_{em} after grinding (nm)	Shift of emission maximum (nm)
7 a	486	490	+ 4
7 b	474	507	+ 31
7 c	571	512	- 59
7 d	473	491	+ 18

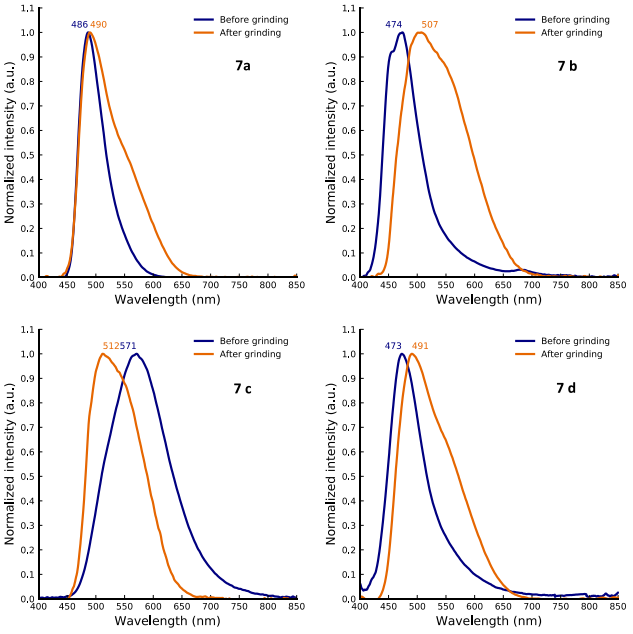

Figure 7. Normalized emission spectra (λ_{ex} = 365 nm) of crystals **7 a-d** before and after grinding.

For compounds **7 a-d,** their mechanofluorochromic properties were also studied. For this purpose, crystals **7 a-d** were grinded and their fluorescent properties were reinvestigated. As can be seen from the fluorescence spectra presented in Figure 7, the fluorescence maxima of compounds **7 a,b,d** after grinding are red-shifted by 4, 31 and 18 nm, respectively (Table 5). This shift can be explained by the appearance of a package where only phenyl rings overlap.[66] In case of **7 c,** the fluorescence maximum shifts in the blue region by 59 nm. The difference in the direction of maximum shifts between **7 a,b,d** and **7 c** can be explained by the assumption that mechanical stress and the transition into an amorphous state lead to the appearance of new packages with varying degrees of overlap. After grinding, the $DBMBF_2$ fragments in **7 a,b,d** have a greater freedom of rotation for the formation of fluorescent excimers. In contrast, **7 c** exhibits a blue-shifted fluorescence after grinding, which may be connected with the destruction of the ground state structures, which are

characterized by the highest degree of overlap. These assumptions correlate well with obtained XRD) patterns (Figure S101, Supporting Information). (Figure S101, Supporting information).

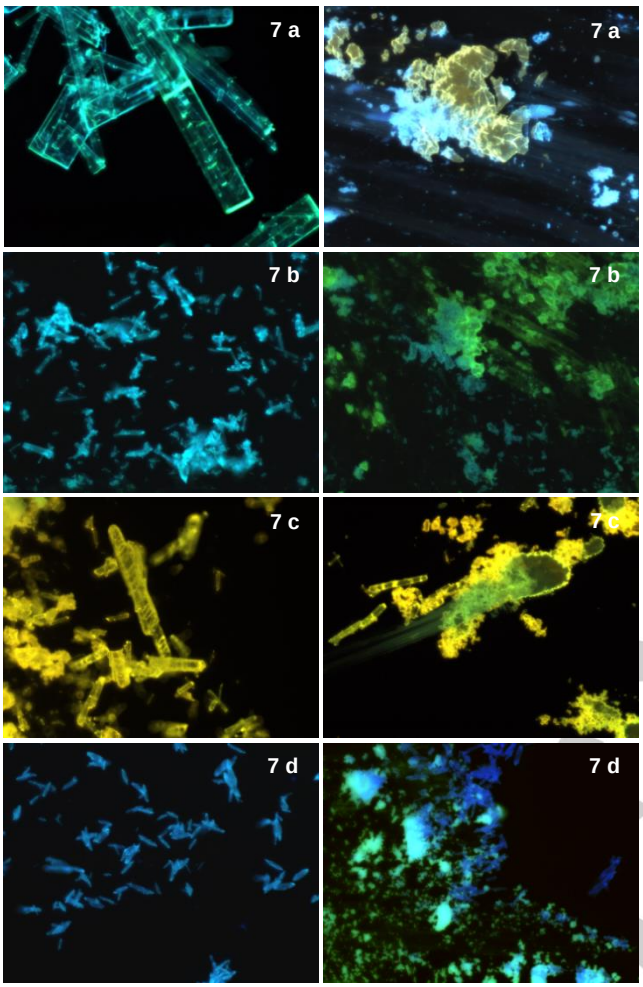

Figure 8. Fluorescence microscope images of crystals **7 a-d** before (left) and after grinding (right). Size of the images is 700 x 1000 μm.

The ability of compounds **7 a-d** to relaxation in the initial state after grinding was investigated and kinetics of this process was studied (Figure 9). It was found that only **7 a** exhibits external stimuli-responsive self-reversible solid-state fluorescence. Figure 9 shows solid state fluorescence spectra of **7 a** for various periods of time after grinding. As can be seen in Figure 9, immediately after grinding a long-wavelength shoulder around 560 nm is observed in the spectrum. The shoulder slowly disappears within 100 minutes and the solid-state fluorescence of **7 a** completely restored in a few hours at room temperature. Figure 10 shows the fluorescence microscopy images of crystals **7 a** for 5 min after mechanical grinding at room temperature. Figure 9 demonstrates changes in solid state fluorescence spectrum observed after grinding of **7 b**. The main changes in the shape of the spectral band for **7 b** are observed immediately

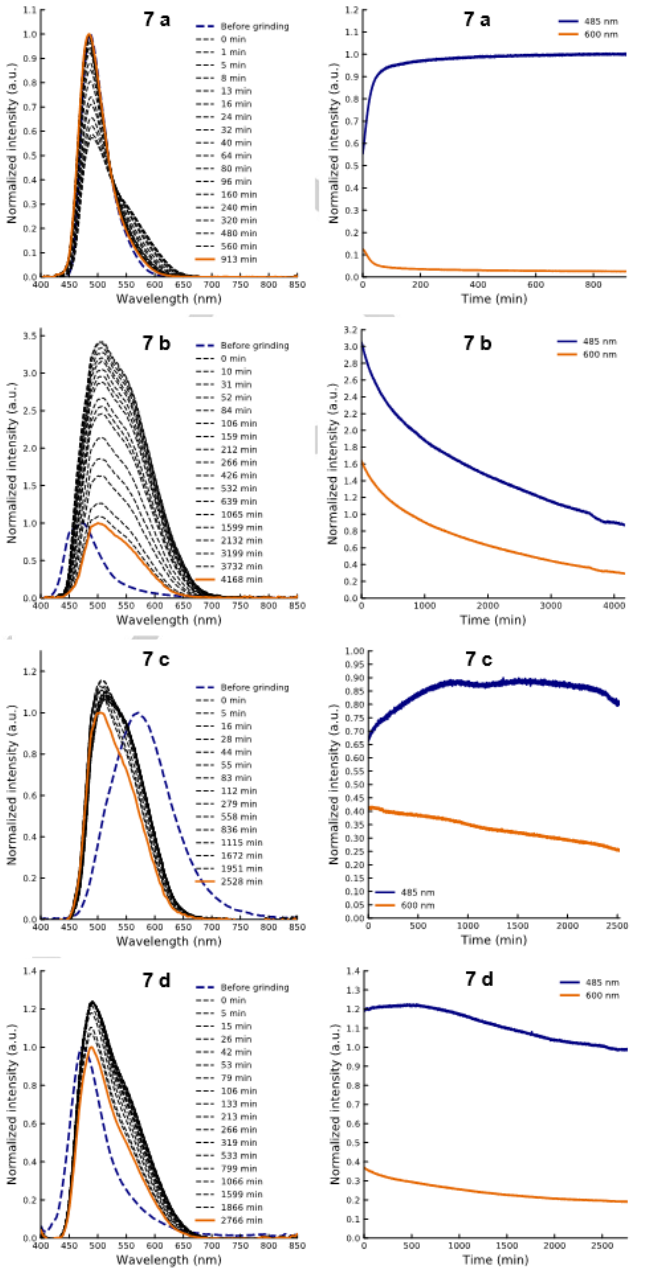

Figure 9. Solid-state fluorescence spectra during time (left) and kinetics of solid-state fluorescence intensity (right) of crystals **7 a-d** after grinding.

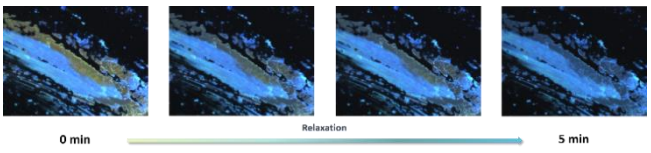

Figure 10. Fluorescence microscopy images of crystals **7 a** for 5 min after mechanical grinding at room temperature.

after grinding. Further observations during 4000 minutes reveal only decrease of integral intensity without significant changes in the line shape. The kinetics of solid-state fluorescence intensity of **7 b** at 485 and 600 nm presented in Figure 9 show almost exponential decay. In the case of **7 c** the solid-state fluorescence spectrum shifts toward shorter wavelengths, in contrast to other compounds and observed changes can be divided into two stages. At first, a gradually blue shift and an increase of intensity during 1000 minutes are observed. This step corresponds to an increase in fluorescent intensity at 485 nm. After this, there is only a decrease in fluorescence intensity without any spectral shape and position changes. As shown in Figure 9, a blue shift of fluorescence maximum is observed for **7 d** after grinding. The spectrum becomes similar to **7 a**. Upon further observation the shoulder peak at 560 nm slowly decreases during 700 minutes. This process corresponds to a plateau in the kinetic curve for fluorescence intensity at 485 nm. After this, the fluorescence intensity gradually decreases without any changes in the spectral shape. The main features that were observed in the solid-state fluorescence after grinding for all compounds **7 a-d** are maximum at about 490 nm and 560 nm.

Conclusions

In summary, a series of novel silicon-centered dendritic $DBMBF_2$ derivatives were synthesized and studied. In solution, the molar extinction coefficients of the sensitized compounds increase with increasing the number of $DBMBF_2$ fragments, while the fluorescence quantum yields and lifetimes slightly decrease. The observed changes are attributed to increasing the rate constants of the non-radiative processes, while the radiative constants remain almost the same and close to the value obtained for $DBMBF_2$. In the solid state, their absorption and emission spectra depend on the size of microcrystals. Tris-$DBMBF_2$ derivative forms fully overlapping dimeric structures exhibiting excimer-like fluorescence, which is well predicted by the quantum-chemical calculations. Mono-$DBMBF_2$ derivative exhibits fully reverse mechanofluorochromic behavior. These results may be useful at the development of active components for pressure sensitive materials. Further research will focus on the development of sensor devices based on these novel $DBMBF_2$-containing building blocks and on investigations of optical properties of their excited dimers and multimers in the crystalline state.

Experimental Section

Experimental details, ^{1}H, ^{13}C, ^{19}F, ^{29}Si NMR, IR spectroscopic and MS data for all compounds, absorbance and fluorescence spectra in solution and X-ray analysis data are given in the supporting information.

Acknowledgements

This study was supported by the Russian Science Foundation (grant no. 18-73-10152). The NMR, IR spectroscopic and X-ray analysis data were obtained using the equipment of Center for molecule composition studies of INEOS RAS. The analysis of fluorescent properties was made using the equipment of the Collaborative Access Center “Center for Polymer Research” of ISPM RAS.

Keywords: crystal engineering • diketonatoboron difluorides • luminescence • mechanofluorochromism • organosilicon compounds

[1] D. Feng, K. Wang, Z. Wei, Y.-P. Chen, C. M. Simon, R. K. Arvapally, R. L. Martin, M. Bosch, T.-F. Liu, S. Fordham, D. Yuan, M. A. Omary, M. Haranczyk, B. Smit, H.-C. Zhou, *Nat. Commun.* **2014**, *5*, 5723.

[2] D. Wang, H. He, X. Chen, S. Feng, Y. Niu, D. Sun, *CrystEngComm* **2010**, *12*, 1041–1043.

[3] R. P. Davies, R. J. Less, P. D. Lickiss, K. Robertson, A. J. P. White, *Inorg. Chem.* **2008**, *47*, 9958–9964.

[4] N. C. Duncan, B. P. Hay, E. W. Hagaman, R. Custelcean, *Tetrahedron* **2012**, *68*, 53–64.

[5] M. Rose, N. Klein, W. Böhlmann, B. Böhringer, S. Fichtner, S. Kaskel, *Soft Matter* **2010**, *6*, 3918.

[6] M. Rose, W. Böhlmann, M. Sabo, S. Kaskel, *Chem. Commun.* **2008**, 2462.

[7] H. Yu, C. Shen, M. Tian, J. Qu, Z. Wang, *Macromolecules* **2012**, *45*, 5140–5150.

[8] B. Zhang, Z. Wang, *Chem. Commun.* **2009**, 5027.

[9] B. Zhang, Z. Wang, *Chem. Mater.* **2010**, *22*, 2780–2789.

[10] Y. Yang, B. Beele, J. Blümel, *J. Am. Chem. Soc.* **2008**, *130*, 3771–3773.

[11] B. Beele, J. Guenther, M. Perera, M. Stach, T. Oeser, J. Blümel, *New J. Chem.* **2010**, *34*, 2729.

[12] J. H. Baker, N. Bhuvanesh, J. Blümel, *J. Organomet. Chem.* **2017**, *847*, 193–203.

[13] U. Stoeck, G. Nickerl, U. Burkhardt, I. Senkovska, S. Kaskel, *J. Am. Chem. Soc.* **2012**, *134*, 17335–17337.

[14] M. Rose, A. Notzon, M. Heitbaum, G. Nickerl, S. Paasch, E. Brunner, F. Glorius, S. Kaskel, *Chem. Commun.* **2011**, *47*, 4814.

[15] C. Pariya, Y. S. Marcos, Y. Zhang, F. R. Fronczek, A. W. Maverick, *Organometallics* **2008**, *27*, 4318–4324.

[16] J. Hierrezuelo, R. Rico, M. Valpuesta, A. Díaz, J. M. López–Romero, M. Rutkis, J. Kreigberga, V. Kampars, M. Algarra, *Tetrahedron* **2013**, *69*, 3465–3474.

[17] Y. Shirai, J. M. Guerrero, T. Sasaki, T. He, H. Ding, G. Vives, B.-C. Yu, L. Cheng, A. K. Flatt, P. G. Taylor, Y. Gao, J. M. Tour, *J. Org. Chem.* **2009**, *74*, 7885–7897.

[18] Y. Yao, J. M. Tour, *J. Org. Chem.* **1999**, *64*, 1968–1971.

[19] J. Hierrezuelo, E. Guillén, J. M. López-Romero, R. Rico, M. R. López-Ramírez, J. C. Otero, C. Cai, *European J. Org. Chem.* **2010**, *2010*, 5672–5680.

[20] J. You, G. Li, Z. Wang, *RSC Adv.* **2012**, *2*, 9488.

[21] H. Lang, Z. Ishtaiwi, T. Rüffer, R. Mothes, B. Walfort, *J. Organomet.*

Chem. **2011**, *696*, 1409–1415.

[22] Y. N. Luponosov, S. A. Ponomarenko, N. M. Surin, O. V. Borshchev, E. A. Shumilkina, A. M. Muzafarov, *Chem. Mater.* **2009**, *21*, 447–455.

[23] L. Wang, D. Wang, H. Wang, S. Feng, *J. Organomet. Chem.* **2014**, *767*, 40–45.

[24] G. Huang, C. Yang, Z. Xu, H. Wu, J. Li, M. Zeller, A. D. Hunter, S. S.-Y. Chui, C.-M. Che, *Chem. Mater.* **2009**, *21*, 541–546.

[25] H. Lu, Q. Wang, L. Gai, Z. Li, Y. Deng, X. Xiao, G. Lai, Z. Shen, *Chem. - A Eur. J.* **2012**, *18*, 7852–7861.

[26] H. Hanamura, R. Haneishi, N. Nemoto, *Tetrahedron Lett.* **2011**, *52*, 4039–4041.

[27] T. Agouâ□‰, M. â. D. Hossainâ□‰, T. Kawashima, *Chem. - A Eur. J.* **2010**, *16*, 368–375.

[28] H.-F. Huang, S.-H. Xu, Y.-B. He, C.-C. Zhu, H.-L. Fan, X.-H. Zhou, X.-C. Gao, Y.-F. Dai, *Dye. Pigment.* **2013**, *96*, 705–713.

[29] D. Hu, F. Shen, H. Liu, P. Lu, Y. Lv, D. Liu, Y. Ma, *Chem. Commun.* **2012**, *48*, 3015.

[30] M. Leung, W.-H. Yang, C.-N. Chuang, J.-H. Lee, C.-F. Lin, M.-K. Wei, Y.-H. Liu, *Org. Lett.* **2012**, *14*, 4986–4989.

[31] S.-O. Kim, Q. Zhao, K. Thangaraju, J. J. Kim, Y.-H. Kim, S.-K. Kwon, *Dye. Pigment.* **2011**, *90*, 139–145.

[32] C.-H. Fan, P. Sun, T.-H. Su, C.-H. Cheng, *Adv. Mater.* **2011**, *23*, 2981–2985.

[33] S. A. Ponomarenko, S. Kirchmeyer, in *Adv. Polym. Sci.*, **2011**, pp. 33–110.

[34] D. Wang, Y. Niu, Y. Wang, J. Han, S. Feng, *J. Organomet. Chem.* **2010**, *695*, 2329–2337.

[35] L. Xiao, Z. Chen, B. Qu, J. Luo, S. Kong, Q. Gong, J. Kido, *Adv. Mater.* **2011**, *23*, 926–952.

[36] W. Wei, P. I. Djurovich, M. E. Thompson, *Chem. Mater.* **2010**, *22*, 1724–1731.

[37] T. Fei, G. Cheng, D. Hu, W. Dong, P. Lu, Y. Ma, *J. Polym. Sci. Part A Polym. Chem.* **2010**, *48*, 1859–1865.

[38] W.-S. Han, H.-J. Son, K.-R. Wee, K.-T. Min, S. Kwon, I.-H. Suh, S.-H. Choi, D. H. Jung, S. O. Kang, *J. Phys. Chem. C* **2009**, *113*, 19686–19693.

[39] D. Hu, P. Lu, C. Wang, H. Liu, H. Wang, Z. Wang, T. Fei, X. Gu, Y. Ma, *J. Mater. Chem.* **2009**, *19*, 6143.

[40] L. Xiao, S.-J. Su, Y. Agata, H. Lan, J. Kido, *Adv. Mater.* **2009**, *21*, 1271–1274.

[41] Y.-Y. Lyu, J. Kwak, W. S. Jeon, Y. Byun, H. S. Lee, D. Kim, C. Lee, K. Char, *Adv. Funct. Mater.* **2009**, *19*, 420–427.

[42] T. Fei, G. Cheng, D. Hu, P. Lu, Y. Ma, *J. Polym. Sci. Part A Polym. Chem.* **2009**, *47*, 4784–4792.

[43] H.-C. Yeh, C.-H. Chien, P.-I. Shih, M.-C. Yuan, C.-F. Shu, *Macromolecules* **2008**, *41*, 3801–3807.

[44] S.-B. Zhao, P. Wucher, Z. M. Hudson, T. M. McCormick, X.-Y. Liu, S. Wang, X.-D. Feng, Z.-H. Lu, *Organometallics* **2008**, *27*, 6446–6456.

[45] Q. Shen, S. Ye, G. Yu, P. Lu, Y. Liu, *Synth. Met.* **2008**, *158*, 1054–1058.

[46] P.-Z. Chen, L.-Y. Niu, Y.-Z. Chen, Q.-Z. Yang, *Coord. Chem. Rev.* **2017**, *350*, 196–216.

[47] K. Tanaka, Y. Chujo, *NPG Asia Mater.* **2015**, *7*, e223–e223.

[48] A. Loudet, K. Burgess, *Chem. Rev.* **2007**, *107*, 4891–4932.

[49] R. Yoshii, K. Suenaga, K. Tanaka, Y. Chujo, *Chem. - A Eur. J.* **2015**, *21*, 7231–7237.

[50] Z. Zhang, Z. Wu, J. Sun, B. Yao, G. Zhang, P. Xue, R. Lu, *J. Mater. Chem. C* **2015**, *3*, 4921–4932.

[51] T. Sagawa, F. Ito, A. Sakai, Y. Ogata, K. Tanaka, H. Ikeda, *Photochem. Photobiol. Sci.* **2016**, *15*, 420–430.

[52] N. Boens, V. Leen, W. Dehaen, *Chem. Soc. Rev.* **2012**, *41*, 1130–1172.

[53] D. Ionov, G. Yurasik, Y. Kononevich, V. Sazhnikov, A. Muzafarov, M. Alfimov, *Procedia Eng.* **2016**, *168*, 341–345.

[54] D. S. Ionov, G. A. Yurasik, Y. N. Kononevich, N. M. Surin, E. A. Svidchenko, V. A. Sazhnikov, A. M. Muzafarov, M. V. Alfimov, *Nanotechnologies Russ.* **2017**, *12*, 338–351.

[55] Y. N. Kononevich, V. A. Sazhnikov, A. S. Belova, A. A. Korlyukov, A. D. Volodin, A. A. Safonov, G. A. Yurasik, D. S. Ionov, A. M. Muzafarov, *New J. Chem.* **2019**, *43*, 13725–13734.

[56] D. S. Ionov, V. A. Sazhnikov, G. A. Yurasik, A. A. Safonov, Y. N. Kononevich, M. V. Alfimov, *High Energy Chem.* **2018**, *52*, 485–491.

[57] Y. N. Kononevich, N. M. Surin, V. A. Sazhnikov, E. A. Svidchenko, V. M. Aristarkhov, A. A. Safonov, A. A. Bagaturyants, M. V. Alfimov, A. M. Muzafarov, *Spectrochim. Acta Part A Mol. Biomol. Spectrosc.* **2017**, *175*, 177–184.

[58] D. S. Ionov, G. A. Yurasik, S. P. Molchanov, V. A. Sazhnikov, V. M. Aristarkhov, Y. N. Kononevich, I. B. Meshkov, N. V. Voronina, A. M. Muzafarov, M. V. Alfimov, *Nanotechnologies Russ.* **2016**, *11*, 444–453.

[59] D. S. Ionov, V. A. Sazhnikov, G. A. Yurasik, A. V. Antonov, Y. N. Kononevich, M. V. Alfimov, *High Energy Chem.* **2015**, *49*, 183–188.

[60] T. M. Schmidt, V. E. Bochenkov, J. D. A. Espinoza, E. C. P. Smits, A. M. Muzafarov, Y. N. Kononevich, D. S. Sutherland, *J. Phys. Chem. C* **2014**, *118*, 2138–2145.

[61] J. D. Arias Espinoza, V. Sazhnikov, E. C. P. Smits, D. Ionov, Y. Kononevich, I. Yakimets, M. Alfimov, H. F. M. Schoo, *J. Fluoresc.* **2014**, *24*, 1735–1744.

[62] P. S. Rukin, A. Y. Freidzon, A. V. Scherbinin, V. A. Sazhnikov, A. A. Bagaturyants, M. V. Alfimov, *Phys. Chem. Chem. Phys.* **2015**, *17*, 16997–17006.

[63] T. O. O. Harju, J. Erostyák, Y. L. L. Chow, J. E. I. E. I. Korppi-Tommola, *Chem. Phys.* **1994**, *181*, 259–270.

[64] T. O. Harju, J. E. I. Korppi-tommola, a H. Huizer, C. a G. O. Varma, *J. Phys. Chem.* **1996**, *100*, 3592–3600.

[65] M. Tanaka, E. Ohta, A. Sakai, Y. Yoshimoto, K. Mizuno, H. Ikeda, *Tetrahedron Lett.* **2013**, *54*, 4380–4384.

[66] A. Sakai, E. Ohta, Y. Yoshimoto, M. Tanaka, Y. Matsui, K. Mizuno, H. Ikeda, *Chem. - A Eur. J.* **2015**, *21*, 18128–18137.

[67] T. Hinoue, Y. Shigenoi, M. Sugino, Y. Mizobe, I. Hisaki, M. Miyata, N. Tohnai, *Chem. - A Eur. J.* **2012**, *18*, 4634–4643.

[68] A. A. Safonov, A. A. Bagaturyants, V. A. Sazhnikov, *J. Mol. Model.* **2017**, *23*, 164.

[69] A. Sakai, M. Tanaka, E. Ohta, Y. Yoshimoto, K. Mizuno, H. Ikeda, *Tetrahedron Lett.* **2012**, *53*, 4138–4141.

Entry for the Table of Contents

FULL PAPER

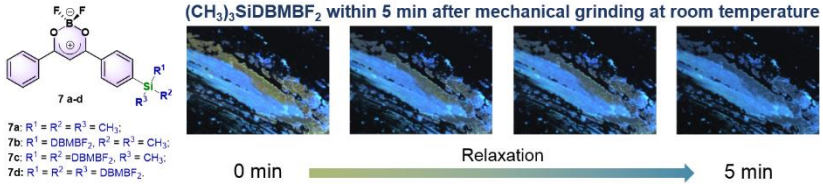

Four novel tetrahedral silicon-centered derivatives of dibenzoylmethanatoboron difluoride ($DBMBF_2$) were synthesized and characterized. Tris-$DBMBF_2$ derivative forms fully overlapping dimeric structures exhibiting excimer-like fluorescence. Mono-$DBMBF_2$ derivative exhibits fully reverse mechanofluorochromic behavior.

Yuriy N. Kononevich, Maxim N. Temnikov, Alexander A. Korlyukov, Alexander D. Volodin, Pavel V. Dorovatovskii, Viacheslav A. Sazhnikov, Andrey A. Safonov, Dmitriy S. Ionov, Anatoly A. Ivanov, Nikolay M. Surin, Evgeniya A. Svidchenko, and Aziz M. Muzafarov **

Page No. – Page No.

Tetrahedral Silicon-Centered Dibenzoylmethanatoboron Difluorides: Synthesis, Crystal Structure and Photophysical Behavior in Solution and Solid State